JOURNAL OF MATERIALS SCIENCE 27 (1992) 6357–6364

Proton conducting polymer electrolyte: II poly ethylene oxide + NH_4I system

K. K. MAURYA, NEELAM SRIVASTAVA, S. A. HASHMI, S. CHANDRA*
Department of Physics, Banaras Hindu University, Varanasi 221 005, INDIA

A new proton conducting polymer electrolyte PEO + NH_4I system has been investigated. The solution-cast films of different stochiometric ratios have been prepared and characterized. Proton transport has been established using various experimental studies, namely optical microscopy, X-ray diffraction, differential thermal analysis, infrared, coulometry transient ionic current and electrical conductivity measurements at different temperatures and humidity. The maximum conductivity of the complexed material has been found to be $\sim 10^{-5}$ S cm^{-1}. Both H^+ ion and I^- anion movements are involved with respective transference numbers and mobilities as $t_{H^+} = 0.74$, $t_{I^-} = 0.09$, $\mu_{H^+} = 4.97 \times 10^{-6}$ cm^2 V^{-1} s^{-1} and $\mu_{I^-} = 7.65 \times 10^{-7}$ cm^2 V^{-1} s^{-1}.

1. Introduction

The ion-conducting polymer electrolytes have attracted wide interest after the pioneering work by the groups of Wright [1, 2] and Armand [3, 4] in the 1970s. The ionically conducting polymer electrolytes are mostly of alkali ions such as Li^+ and Na^+ (for reviews see [5–8]). Recently it has been realized that developing proton (H^+) ion conductors have vast technological applications, particularly in fuel cells. Some, but very few, proton conducting polymer electrolytes have been reported so far, e.g. polyethylene oxide (PEO):NH_4SCN and $NH_4SO_3CF_3$ [9], PEO and poly acrylic acid (PAA):NH_4HSO_4 [10], PEO:NH_4ClO_4 [11, 12], PEO:H_3PO_4 [13], poly vinyl alcohol (PVA):H_3PO_4 [14, 15] poly ethylene imine (PEI):H_2SO_4 and H_3PO_4 [16], HCl [17], CH_3COOH [18]. In general, it is difficult to establish the proton conduction unambiguously. In the present paper, we report a new proton conducting polymer electrolyte obtained by complexing PEO polymer with NH_4I. A wide variety of experiments (X-ray diffraction, differential thermal analysis, infrared, complex impedance analysis for conductivity, σ versus $1/T$, σ versus relative humidity, transference number, mobility) have been carried to establish proton transport and to characterize the material.

It has been observed from the above studies that the PEO + NH_4I system is predominantly an H^+ ion conductor together with a small contribution to the total conductivity due to the I^- motion.

2. Experimental procedure

Films ($\sim$ 200–400 μm) of PEO (mol. wt 600 000) complexed with NH_4I were prepared of different compositions, i.e. NH_4^+/EO ratios varying from $\sim$0.016–0.138. The stoichiometric ratio of different compositions was solution cast followed by slow evaporation. Distilled methanol was used as solvent. The films were dried rigorously in a high vacuum to eliminate all traces of methanol (confirmed by infrared studies).

Optical micrographs of the films of different compositions were taken using a Leitz optical microscope (LABORLUX "D"). The X-ray diffraction (XRD) studies were carried out using Philips X-ray diffractometer (PW 1710). The infrared (IR) spectral study of the films of pure PEO and complexed PEO of different compositions was carried out using a Perkin–Elmer IR spectrophotometer (Model 883). Differential thermal analysis (DTA) was carried out using Linseis instruments (Type 2045). Samples of $\sim$ 60 mg of each composition were kept in a platinum crucible and heated in a static air atmosphere at a heating rate of 5° C min^{-1}.

The total ionic transference number was computed using the polarization method. In this method, the d.c. current was monitored as a function of time, on application of a fixed d.c. voltage across the cell Al/PEO + NH_4I electrolyte/Al. The transference number, t_{ion}, was calculated from the initial current, i_i, and final residual current, i_e, after polarizing the electrolyte, using the formula

$$t_{ion} = (i_i - i_e)/i_i \quad (1)$$

However this method does not give information regarding the cationic/anionic contribution to the total conductivity. To circumvent this problem, a coulometric investigation based on Faraday's law of electrolysis was carried out using a specially designed double-arm coulometer or electrolysis cell. Details of this method is given elsewhere [19, 20]. The gas

* Author to whom all correspondence should be addressed.

0022–2461

collected at the cathode end after coulometry was tested using a gas chromatograph (Tracor Instruments, Model 540).

The transient ionic current (TIC) measurement technique was used to detect the number of different types of mobile ionic species in the bulk and to evaluate their respective mobility. In this method, the sample (thickness 0.18 mm, area 78.54 mm^2), sandwiched between aluminium electrodes, was polarized using a d.c. voltage of 2.0 V. The polarity of the voltage was reversed after about 30 min and the transient ionic current was recorded as a function of time. Details of the experimental technique have been reported elsewhere [21]. The mobility, μ, of mobile ionic species was calculated using the formula

$$\mu = d^2/\tau V \quad (2)$$

where d is the thickness of the sample, V is the voltage applied and τ is time of flight corresponding to the current maxima.

The electrical conductivity of the samples of different compositions (NH_4^+/EO ratio varying from 0–0.130) was measured from $\sim$ 25–150 °C by using complex impedance/admittance plots obtained with the help of a computer (hp 9122) controlled Schlumberger Solartron (1250) frequency response analyser coupled with a Solartron (1286) electrochemical interface. Vacuum-coated aluminium was used as the electrodes.

3. Results and discussion

3.1. Structural studies

3.1.1. Optical microscopy

Optical micrographs of different compositions of PEO and NH_4I are shown in Fig. 1. Large spherulites of different sizes are observed for the composition with NH_4^+/EO ratio = 0.034 (Fig. 1a). This suggests the presence of crystalline complexed material which is also indicated in XRD studies (Section 3.1.2). Some amorphous regions are also seen between the spherulites. These amorphous regions increase and subsequently the spherulitic regions become smaller with increasing concentration of NH_4I in PEO. For the NH_4^+/EO ratio = 0.130, the spherulites disappear. This is indicative of a fast decrease in degree of crystallinity. A quantitative estimation of the degree of crystallinity has been carried out in DTA studies (see Section 3.1.3).

3.1.2. X-ray diffraction studies

The XRD patterns of different compositions are shown in Fig. 2. The following results were obtained.

(i) A comparison of the XRD patterns of the complexed PEO with that of the uncomplexed PEO shows that the broad peaks between $2\theta = 15°$ and 30°, related to the amorphicity of the polymers, are more intense in the complexed PEO compared to the pure PEO. This shows a decrease in degree of crystallinity

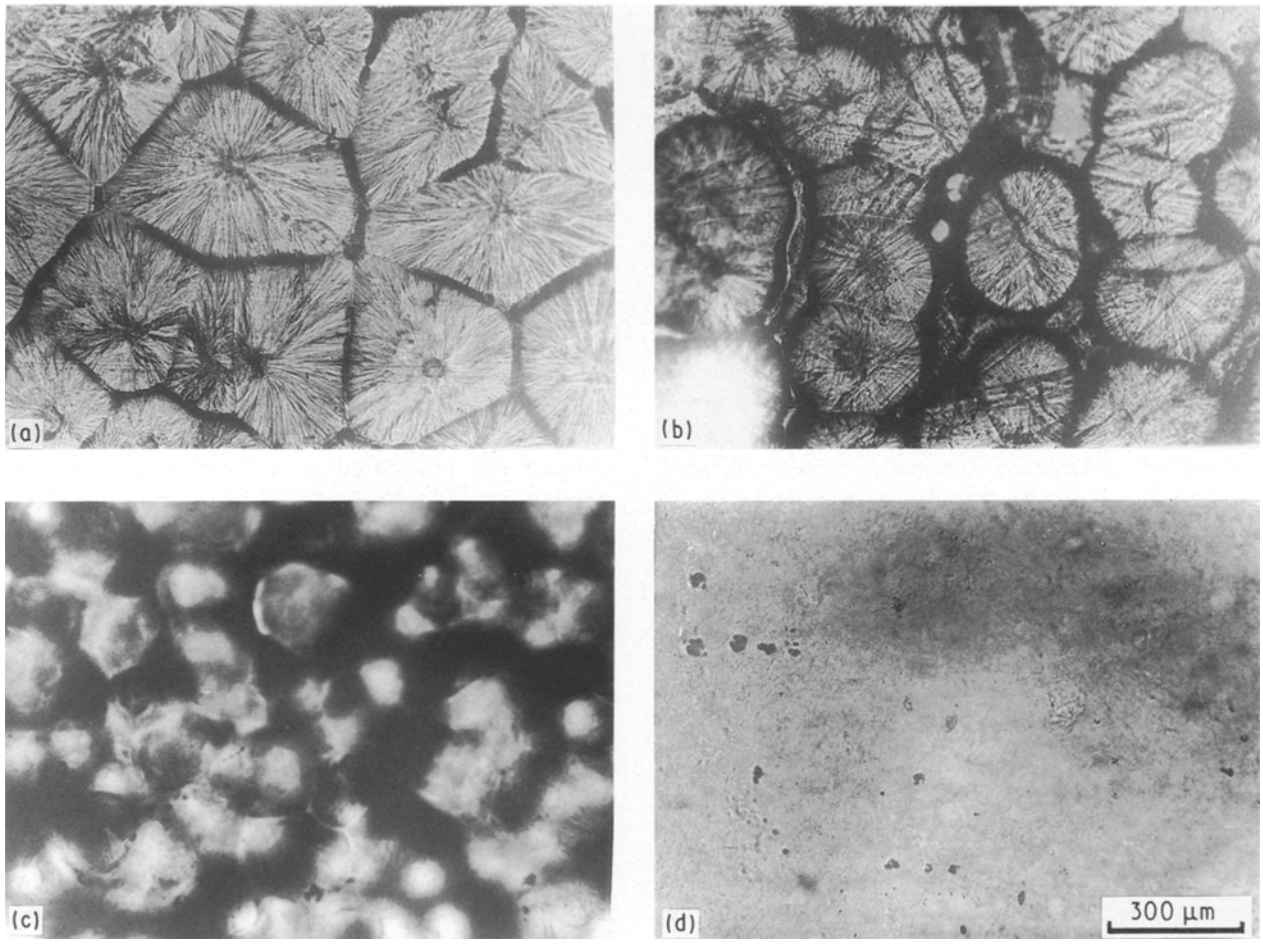

Figure 1 Optical micrographs of PEO + NH_4I systems for NH_4^+/EO ratios (a) 0.034, (b) 0.054, (c) 0.076, and (d) 0.130.

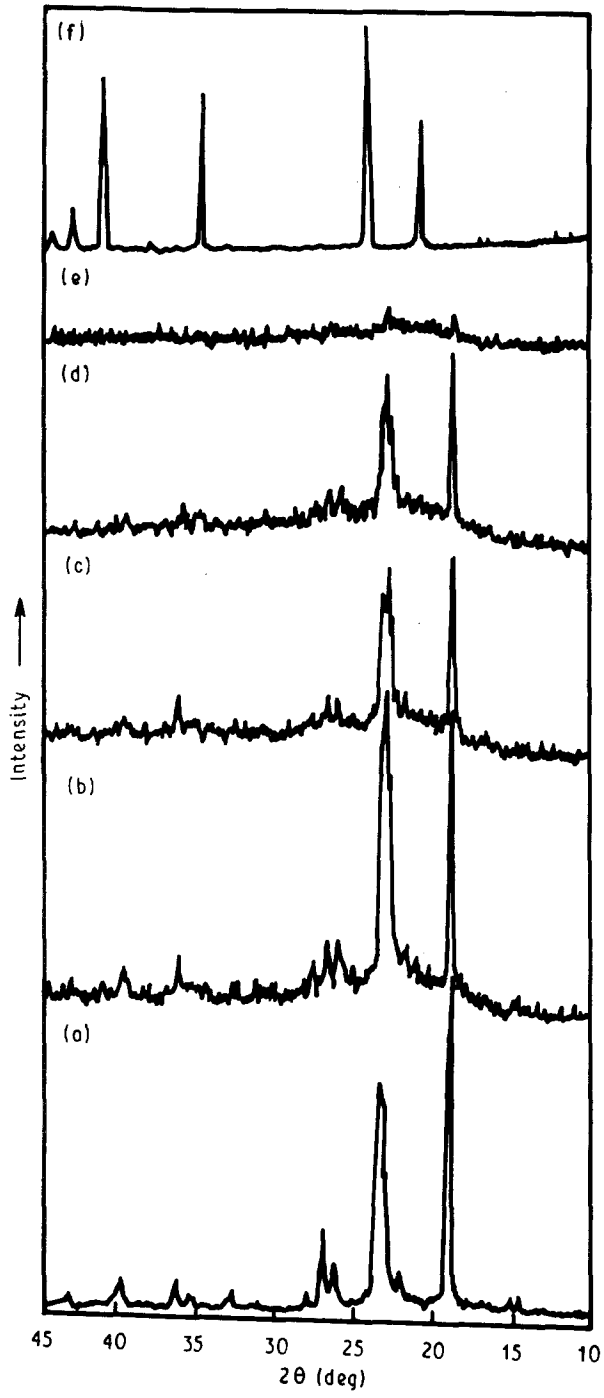

Figure 2 XRD patterns of (a) pure PEO, and complexed PEO with NH_4^+/EO ratios equal to (b) 0.034, (c) 0.054, (d) 0.076, and (e) 0.010, (f) Pure NH_4I.

of the polymer with increasing concentration of NH_4I. The decrease in degree of crystallinity has also been observed in optical microscopic and DTA studies.

(ii) Peaks corresponding to the uncomplexed PEO are also present together with that of the complexed PEO showing the simultaneous presence of both crystalline uncomplexed and complexed PEO.

(iii) Almost no peaks were observed in the complexed material of the NH_4^+/EO ratio $\simeq$ 0.010. This shows the dominant presence of amorphous material after the NH_4^+/EO ratio = 0.010.

(iv) No peak was observed in the complexed material corresponding to pure NH_4I up to the NH_4^+/EO ratio = 0.010. This shows the absence of excess NH_4I (uncomplexed) in the materials.

3.1.3. Differential thermal analysis

DTA curves of pure PEO and complexed PEO of different NH_4^+/EO ratios are shown in Fig. 3. An endothermic peak corresponding to the melting of pure PEO appears at $T_m \simeq 68\,^\circ C$ (Fig. 3a). The main endothermic melting peak of the complexed material of NH_4^+/EO ratio $\simeq$ 0.034 appears at 64 °C (Fig. 3b). The melting point, T_m, is lowered with increasing concentration of NH_4I. The melting enthalpy, ΔH_m, and degree of crystallinity of pure PEO and complexed PEO of each composition have been roughly estimated by comparing the area of the melting peak of the samples with that of paradibromobenzene ($T_m = 87\,^\circ C$, $\Delta H_m = 20.55\,cal\,g^{-1}$) as a standard material. The melting point T_m, melting enthalpy, ΔH_m, and degree of crystallinity are listed in Table I. It is obvious that the degree of crystallinity decreases from 77%; for pure PEO, to 14% for the complexed material with NH_4^+/EO ratio $\simeq$ 0.143. The decrease in degree of crystallinity is also observed in optical microscopy and XRD results.

Apart from the T_m peak in the DTA curve of Fig. 3, two broad endothermic peaks were also observed at $\sim$ 105 and $\sim$ 180 °C for the complexed PEO of NH_4^+/EO ratio = 0.034 (Fig. 3b). The peak at $T_f \simeq 105\,^\circ C$ may be attributed to the complexed

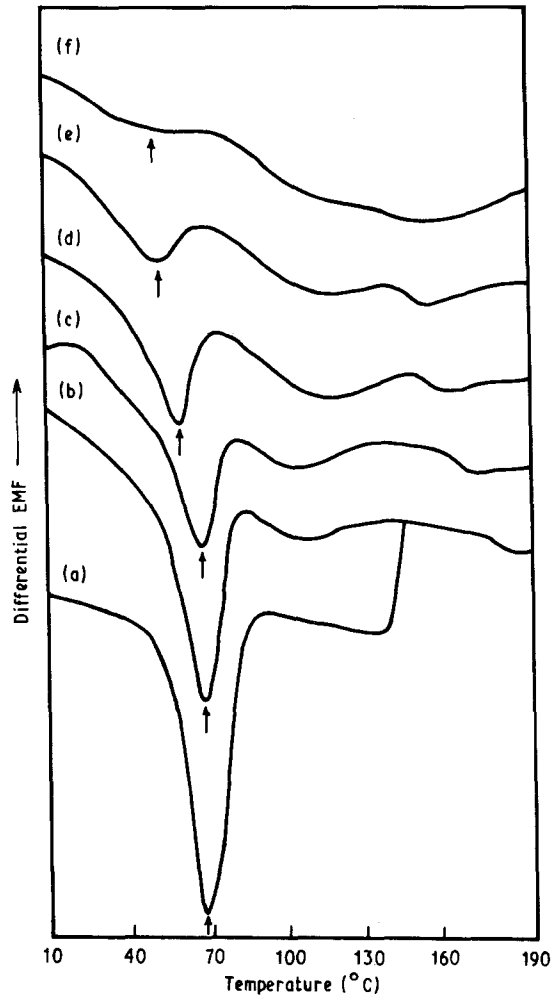

Figure 3 DTA curves of (a) PEO (pure), and–complexed PEO with different NH_4^+/EO ratios: (b) 0.034, (c) 0.054, (d) 0.076, (e) 0.010, (f) 0.130.

TABLE I Melting point, melting enthalpy and degree of crystallinity of PEO + NH_4I systems

PEO + NH_4I (NH_4^+/EO unit)	T_m (°C)	ΔH_m (cal g^{-1})	Crystallinity[a] (%)
PEO	68	34.5	77
0.034	64	25.5	63
0.054	61	16.7	44
0.076	55	13.2	37
0.010	49	8.7	26
0.130	–	4.5	14

[a] Calculated assuming $\Delta H_m = 45$ cal g^{-1} for 100% crystalline PEO [22].

amorphous PEO and that at $T_d \simeq 180$ °C is associated with the dissociation of the material. T_f increases, whereas T_d decreases with increasing concentration of NH_4I.

3.1.4. Infrared studies

The IR spectra of pure PEO, complexed PEO of different compositions and pure NH_4I are shown in Fig. 4. The following general features may be noted.

(a) The IR spectra of complexed PEO do not contain specific bands of NH_4I. This shows that the complexation is complete and no unreacted NH_4I remains.

(b) A shift of ~ 65 cm^{-1} (from 3129 cm^{-1} of pure NH_4I to 3194 cm^{-1} of PEO:NH_4I complex) was observed in the N–H stretching region of NH_4^+ ions after complexation.

(c) The H–N–H bending peak of NH_4^+ at 1393 cm^{-1} also shows a shift towards higher wave number. After the shift, complexation seem to have resulted in splitting into many bands. The high-resolution record of the IR spectra in this wave number region is shown in Fig. 5. It is obvious that the split new peaks at 1428, 1435, 1440 and 1445 cm^{-1} appear in the complexed sample.

The strong shifts in NH_4^+ vibrational bands and their splitting into many bands suggest the complexation of the system or, in other words, the coordination of NH_4^+ ions with ether oxygen of PEO. The conformation of pure PEO and their alkali metal salt complexes has been studied extensively using vibrational spectroscopy [23, 24]. Pure PEO has the *trans*, T (CC-OC), *trans*, T(CO-CC), *gauche*, G(OC-CO) or T_2G conformation. The spectral feature between 1000 and 700 cm^{-1} is very sensitive to any conformational change in PEO. The presence of the 962, 942 and 824 cm^{-1} bands of CH_2 symmetrical and asymmetrical rocking of pure PEO shows the presence of *gauche* conformation of O–[$(CH_2)_2$]–O [23, 24]. Generally, the coordination of alkali metal ions with PEO does not affect the *gauche* conformation of PEO. In some complexes such as PEO–HgO_2, the O–[CH_2]$_2$–O groups are in *trans*, *gauche*-minus as well as *gauche* conformation. In the present PEO + NH_4I system, a comparison of the spectral feature between 1000 and 700 cm^{-1} shows that the bands related to *gauche* conformation of O–[CH_2]$_2$–O of PEO are only present in the complexed material. This suggests that the *gauche* conformation of PEO has not been affected due to the complexation with NH_4I.

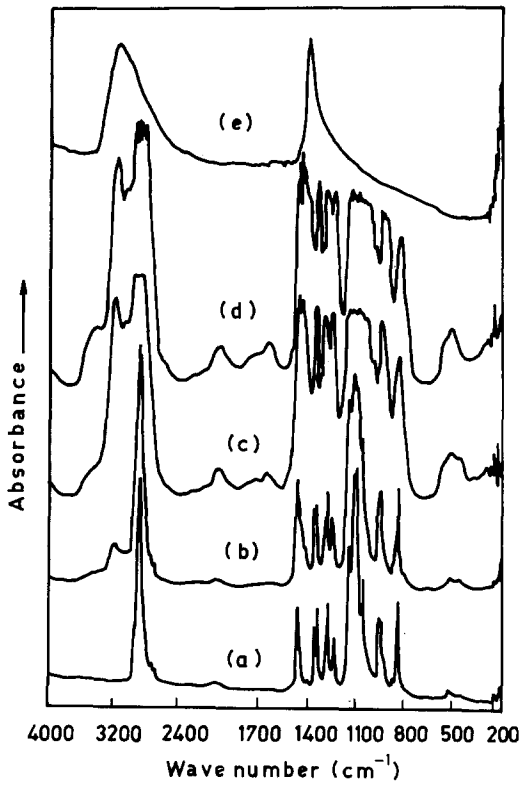

Figure 4 IR absorption spectra of (a) PEO (pure), and complexed PEO with different NH_4^+/EO ratios: (b) 0.034, (c) 0.054, (d) 0.076, (e) pure NH_4I.

3.2. Transport number and mobility

Total ionic transport number of the complexed material of NH_4^+/EO ratio = 0.034 has been measured using the polarization technique. The polarization current versus time plot is shown in Fig. 6. The ionic transport number has been calculated using Equation 1 and is found to be ~ 0.97. This shows that the charge transport in the complex is mainly ionic. To distinguish the cationic and/or anionic contribution to the total ionic transport number, a coulometric investigation was carried out. This method is based on Faraday's law of electrolysis. The following results were obtained.

(a) On passing a constant current (~ 25.5 μA) through the electrolysis cell, in which the polymer sample is sandwiched between mercury electrodes, gases evolve both at the cathode and anode ends. The evolution of cathode-side gas is dominant. The volumes of the gases evolved as a function of charge passed through the cell is shown in Fig. 7.

(b) The gas, collected at the cathode side of the electrolysis cell, was tested using gas chromatography and it was found to be hydrogen. It was difficult to test the gas at the anode side because the amount of gas collected was very small and we had no facilities by which to detect such a small amount of gas. It is possible that the gas evolved at anode is iodine, as a result of the I^- movement in the bulk.

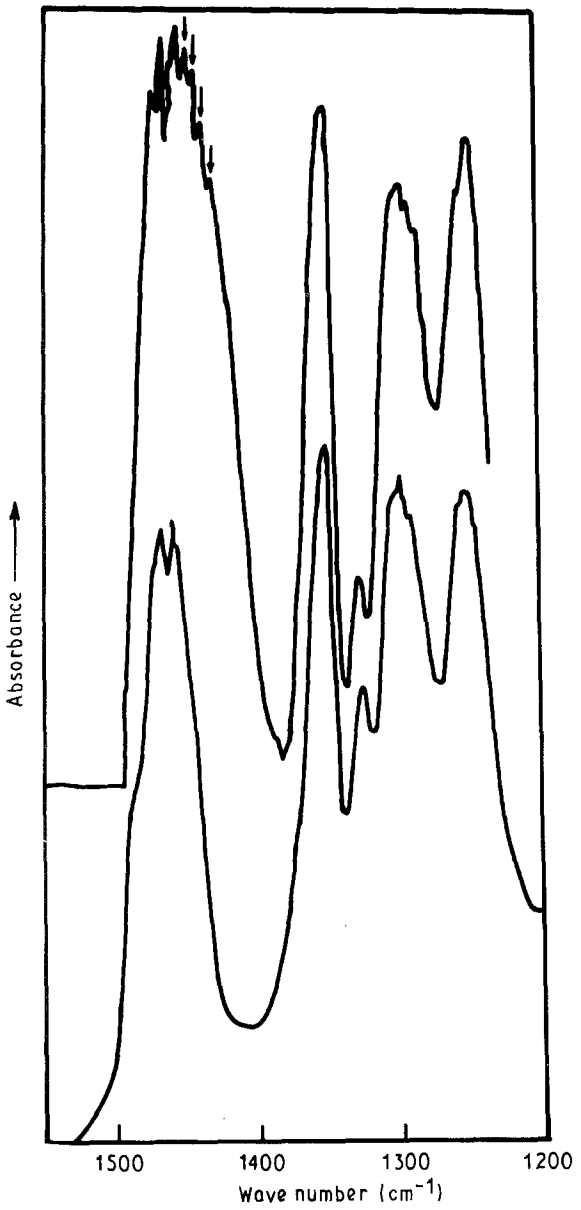

Figure 5 The splitting of NH_4^+ peaks in the IR spectra of (a) pure PEO and (b) complexed PEO for NH_4^+/EO ratio = 0.054.

(c) The transport number for H^+ and I^- ions was calculated separately using the formula

$$t_{H^+/I^-} = \frac{\text{charge passed due to a particular ion}}{\text{total charge passed}} = \frac{2\,(V)_{NTP}\,Ne}{22\,400\,it}. \quad (3)$$

where $(V)_{NTP}$ is the volume (ml) of the H_2/I_2 gas at NTP, N is Avogadro's Number, e is the electronic charge, i the electrolysis current and t is electrolysis time. The transport number for H^+ ions (t_{H^+}) and for I^- ions (t_{I^-}) were found to be ~ 0.74 and ~ 0.09, respectively. The total ionic transport number, t_{ion}, using this method was found to be $t_{ion} = t_{H^+} + t_{I^-} = 0.83$.

(d) A reddish material was found sticking to the anode surface, after electrolysis. This is attributed to the possible formation of HgI_2 at the anode end during the electrolysis in the coulometer, following the reaction

$$Hg + 2I^- \rightarrow HgI_2 + 2e^- \text{ at the anode} \quad (4)$$

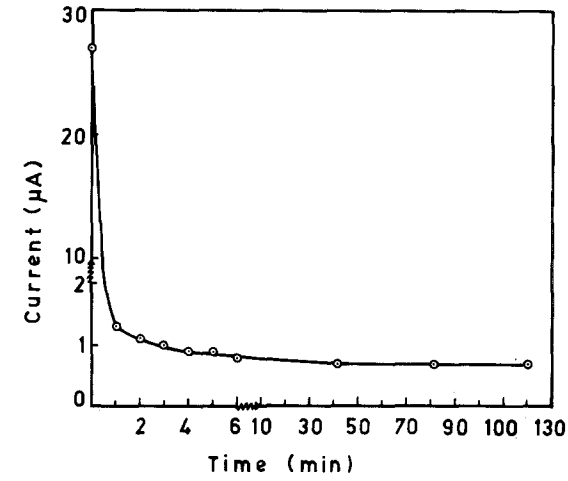

Figure 6 Polarization current–time plot for the complexed PEO with NH_4^+/EO ratio = 0.034 (sample thickness = 0.025 cm, area = 0.785 cm^2 and voltage applied = 1.5 V).

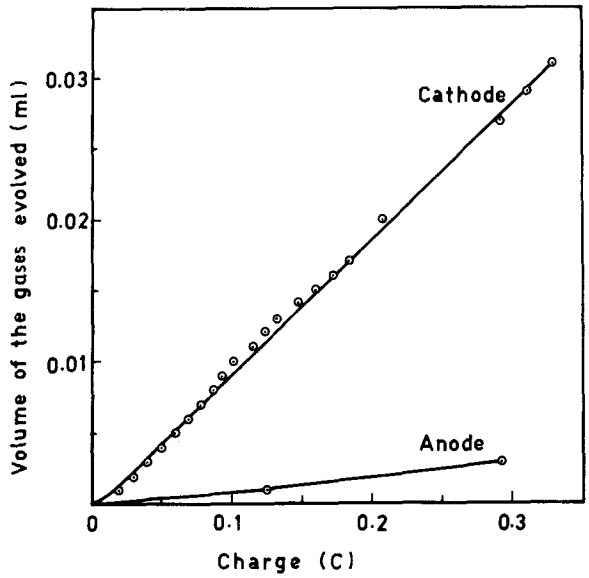

Figure 7 Volume of gases evolved in the double-arm coulometer as a function of charge passed for the complexed sample with NH_4^+/EO = 0.034.

Some of the I^- ions transported out are consumed in the formation of HgI_2, which may lead to an underestimation of the I^- transport number and, subsequently, to the underestimation of the total ionic transport number, mentioned above.

The evolution of a relatively large amount of hydrogen gas at the cathode end and the large value of H^+ ion transport number ($t_{H^+} = 0.74$) suggest that the charge transport in the bulk of the complexed material is mainly protonic.

Mobility of the mobile ionic species (H^+ and I^- ions) was measured using the transient ionic current measurement method. Two peaks were observed in the transient ionic current versus time plot (Fig. 8) corresponding to the two mobile ionic species (H^+ and I^-). Using Equation 2, the mobilities were calculated and were found to be $\mu_1 = 4.97 \times 10^{-6}$ cm^2 $V^{-1}s^{-1}$ and $\mu_2 = 7.65 \times 10^{-7}$ cm^2 $V^{-1}s^{-1}$. It is difficult to identify unambiguously the ionic species associated with μ_1 and μ_2. However, on the basis of ionic

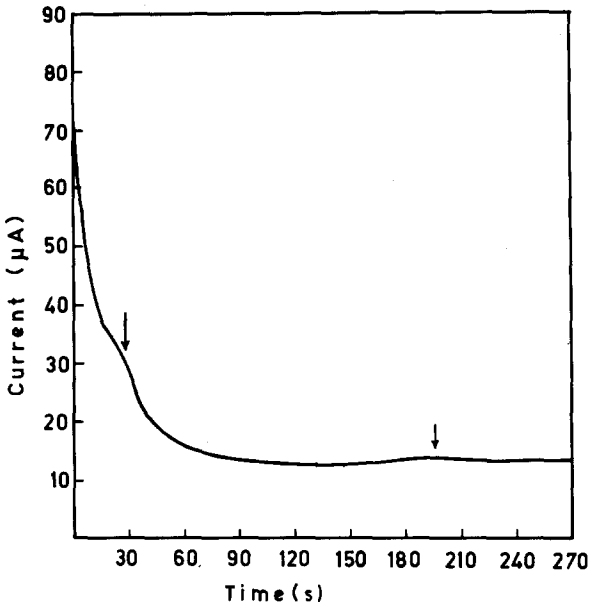

Figure 8 Transient ionic current–time plot for the complexed PEO with NH_4^+/EO ratio = 0.034 (sample thickness = 0.018 cm, voltage applied = 2.0 V).

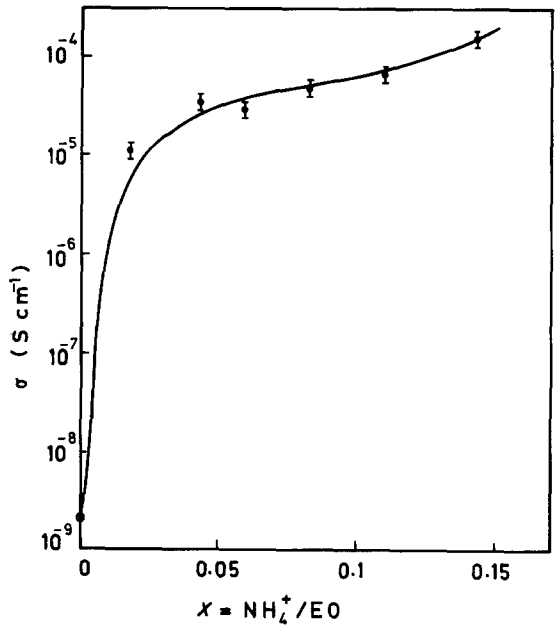

Figure 9 Composition dependence of the electrical conductivity at room temperature (~ 22.5 °C) and relative humidity ~ 60%.

sizes, μ_1 and μ_2 can be assumed to be associated with H^+ and I^-, respectively.

3.3. Electrical conductivity

3.3.1. Composition dependence

The variation of electrical conductivity, σ, as a function of the composition, i.e. the NH_4^+/EO ratio, as shown in Fig. 9. The conductivity of pure PEO is ~ 10^{-9} S cm^{-1} and it increases sharply to ~ 10^{-5} S cm^{-1} on complexing the PEO with NH_4I for NH_4^+/EO ratio = 0.016. The increase in conductivity becomes slower on further addition of NH_4I to PEO. Above the NH_4^+/EO ratio = 0.130, the sample becomes mechanically unstable and it is difficult to make conductivity measurements. It is generally believed that the conductivity increases as the degree of crystallinity decreases or, in other words, the flexibility of the polymeric backbone increases. The continuous increase in conductivity in the present study of the PEO + NH_4I system with increasing NH_4^+/EO ratio has been attributed to the decrease in the degree of crystallinity as observed from the structural studies (Section 3.1).

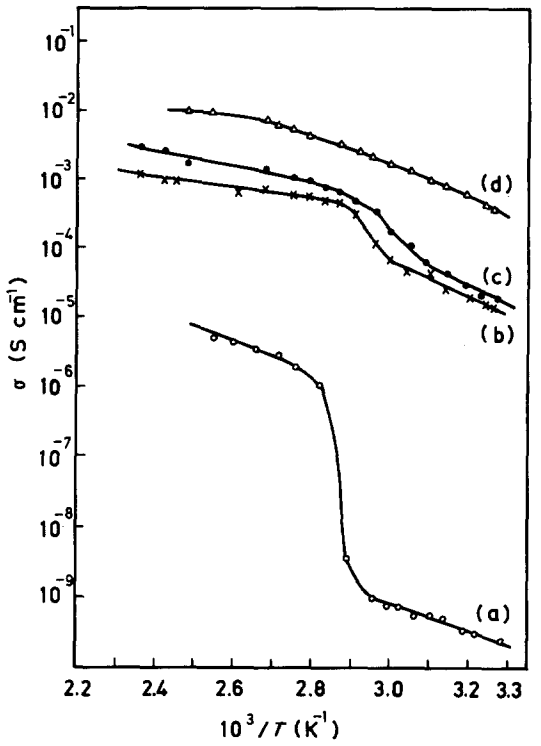

Figure 10 Temperature dependence of the conductivity of (a) pure, and (b–d) complexed PEO: NH_4^+/EO ratios (b) 0.016, (c) 0.076, (d) 0.130.

3.3.2. Temperature dependence

Fig. 10 shows the variation in electrical conductivity of pure PEO and complexes of different compositions as a function of temperature. The temperature dependence of conductivity of polymer–salt complexes follows many patterns, as discussed widely by Ratner [25]. In the present study we found two kinds of pattern.

(i) For a lower concentration of NH_4I in PEO up to NH_4^+/EO ratio ≃ 0.076, the σ–$1/T$ plot follows the Arrhenius behaviour throughout, but with two activation energies above and below the melting point, T_m.

(ii) For a higher concentration of NH_4I, i.e. NH_4^+/EO ≃ 0.013, σ–$1/T$ shows a curvature (Fig. 10d) and follows the Vogel–Tammen–Fulcher (VTF) behaviour throughout the available temperature range.

For each composition with a lower concentration of NH_4I, the conductivity suddenly increases at the melting point. This has been explained on the basis of a semicrystalline to amorphous phase transition. The linear variation in σ–$1/T$ plots before and after T_m

TABLE II Pre-exponential factors and activation energies of the PEO + NH_4I system

NH_4^+/EO ratio	Semicrystalline (before T_m)		Amorphous (after T_m)	
	σ_0 (S cm^{-1})	E_a (eV)	σ_0 (S cm^{-1})	E_a (eV)
PEO pure	9.7×10^{-3}	0.40	8.06×10^{-2}	0.32
0.016	2.6×10^{2}	0.44	1.26×10^{-1}	0.17
0.034	1.15×10^{2}	0.42	7.1×10^{-1}	0.24
0.054	2.23×10^{4}	0.57	6.6×10^{-1}	0.21
0.076	1.96×10^{6}	0.67	1.97	0.24

suggests an Arrhenius–type thermally activated process. The conductivity, σ, may be expressed as

$$\sigma = \sigma_0 \exp(-E_a/kT) \quad (5)$$

where σ_0 is a pre-exponential factor, E_a the activation energy and k is the Boltzmann constant. The calculated values of σ_0 and E_a for different compositions are given in Table II. The values of σ_0 and E_a vary with increasing concentration of NH_4I, both in semicrystalline and amorphous phases. A comparatively larger variation in σ_0 and E_a values has been observed for the semicrystalline phase, than for the amorphous phase. In the semicrystalline phase ($T < T_m$), the activation energy is substantially larger compared to pure PEO (Table II). This would suggest a lower conductivity for complexed materials if σ_0 had remained constant (Equation 5). However, values are higher ($\sim 10^4$ times) for complexed PEO compared to pure PEO (Fig. 8). This enhancement of σ is due to a large increase in the pre-exponential factor, σ_0, as shown in Table II.

For a higher concentration of NH_4I in PEO (i.e. NH_4^+/EO ratio $\sim$ 0.0130), a curvature in the σ–$1/T$ plot has been observed (Fig. 10d). From structural studies, samples of higher NH_4I concentration have been proved to be almost totally amorphous. A curvature in the σ–$1/T$ plot for such an almost amorphous system suggests that the charge transport mechanism can be described using the free volume or VTF theory, in which the segmental motion of the host polymer cooperates with the charge transport. According to the VTF theory, the conductivity, σ, can be expressed as

$$\sigma = AT^{-1/2} \exp[-E_a/k(T - T_0)] \quad (6)$$

The conductivity data have been analysed using the VTF equation (Equation 6) with the adjustable parameters A, E_a and T_0. The non-linear least squares fit to the above equation gives the fitting parameters $A = 1.85$, $E_a = 0.03$ eV and $T_0 = 249$ K.

3.3.3. Humidity dependence

The humidity dependence of the conductivity for the complexed material of NH_4^+/EO ratio = 0.054 is shown in Fig. 11. The conductivity increases ($\sim$ 500 times) when the relative humidity changes from $\sim$ 20% to $\sim$ 80%. This shows a strong humidity dependence of the material. Initially, the conductivity increases sharply and above $\sim$ 60% RH the conductivity becomes almost constant. Above 80% RH the sample becomes molten-like, due to excess swelling of the film, and it is difficult to measure the conductivity.

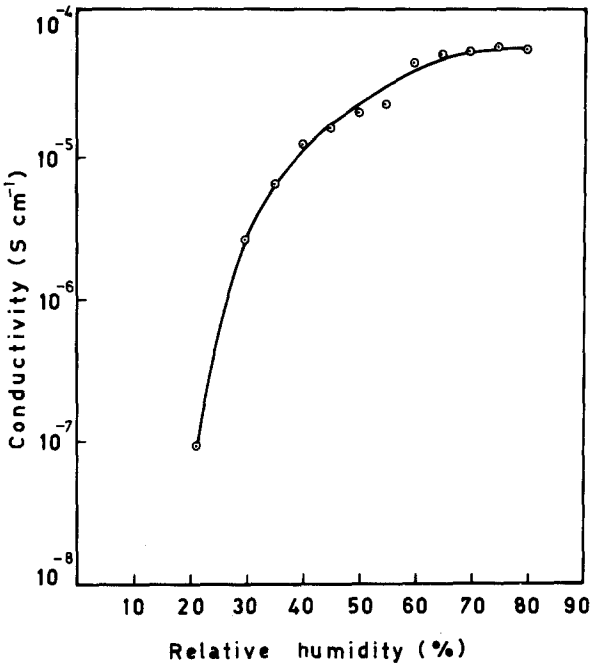

Figure 11 Humidity dependence of the conductivity of the complexed PEO for NH_4^+/EO ratio = 0.054.

4. Conclusion

PEO is shown to form a complex with NH_4I which has a high ionic conductivity. The degree of crystallinity of the complex decreases with increasing concentration of NH_4I. The charge transport is mainly protonic along with I^- movement in the bulk. The respective transference numbers and mobilities are: $t_{H^+} = 0.74$, $t_{I^-} = 0.09$; $\mu_{H^+} = 4.97 \times 01^{-6}$ cm^2 V s^{-1} and $\mu_{I^-} = 7.65 \times 10^{-7}$ cm^2 V^{-1} s^{-1}.

The electrical conductivity of the complexed material has been found to be $\sim 10^{-5}$ S cm^{-1} for the concentration range NH_4^+/EO = 0.016–0.130. For the lower concentration of NH_4I (i.e. NH_4/EO ratio $\simeq$ 0.076), the σ–$1/T$ plot follows an Arrhenius behaviour with two activation energies before and after T_m. The σ–$1/T$ plot for a higher concentration (NH_4^+/EO = 0.130) follows the VTF pattern. Further, the electrical conductivity of PEO: NH_4I complex depends upon the relative humidity of the ambient.

Acknowledgements

We thank the Department of Non-Conventional Energy Sources (Government of India) for financial support. One of us (SAH) thanks CSIR for the award of a Research Associateship.

References

1. P. V. WRIGHT, *Br. Polym. J.* 7 (1975) 319.
2. D. E. FENTON, J. M. PARKER and P. V. WRIGHT, *Polymer* **14** (1973) 589.
3. M. B. ARMAND, J. M. CHABAGNO and M. DUCLOT, in "Fast Ion Transport in Solids", edited by P. Vashishta,

J. N. Mundy and G. K. Shenoy (North Holland, Amsterdam, 1979) p. 131.
4. *Idem*, Extended Abstracts, in "Second International Conference on Solid Electrolytes", St Andrews, Scotland, 1978 (unpublished).
5. J. R. MACCALLUM and C. A. VINCENT (Eds), "Polymer Electrolyte Reviews 1" (Elsevier Applied Science, London, New York, 1987).
6. M. B. ARMAND, *Ann. Rev. Mater. Sci.* **16** (1986) 245.
7. M. A. RATNER and D. F. SHRIVER, *Chem. Rev.* **88** (1988) 109.
8. J. R. OWEN, in "Superionic Solids and Solid Electrolytes – Recent Trends", edited by A. L. Laskar and S. Chandra (Academic Press, New York, 1989).
9. M. STAINER, L. C. HARDY, D. H. WHITMORE and D. F. SHRIVER, *J. Electrochem. Soc.* **131** (1984) 784.
10. M. F. DANIEL, B. DESBAT and J. C. LASSEGUES, *Solid State Ionics* **28–30** (1988) 632.
11. S. A. HASHMI, AJAY KUMAR, K. K. MAURYA and S. CHANDRA, *J. Phys. D. Appl. Phys.* **23** (1990) 1307.
12. S. CHANDRA, S. A. HASHMI and G. PRASAD, *Solid State Ionics* **40/41** (1990) 651.
13. P. DONOSO, W. GORECKI, C. BERTHIER, F. DEFENDINI, C. POINSIGNON and M. B. ARMAND, *ibid.* **28–30** (1988) 969.
14. S. PETTY-WEEKS and A. J. POLAK, *Chem. Engng News* (1985) 28.
15. R. P. SINGH, P. N. GUPTA, S. L. AGRAWAL and U. P. SINGH, "Solid State Ionics", edited by G. Nazyi, R. A. Huggins and D. F. Shriver, Materials Research Society, Pittsburg, PA, USA) p. 361.
16. M. F. DANIEL, B. DESBAT, F. CRUEGE, O. TRINQUET and J. C. LASSEGUES, *Solid State Ionics* **28–30** (1988) 637.
17. Y. CHATANI and T. IRIE, *Polymer* **29** (1988) 2126.
18. Y. CHATANI, Y. YAKURA and T. ISHIOKA, *ibid.* **31** (1990) 208.
19. S. K. TOLPADI, S. CHANDRA and S. A. HASHMI, *Solid State Ionics* **18/19** (1986) 1008.
20. S. CHANDRA, S. K. TOLPADI and S. A. HASHMI, *J. Phys. Condens. Matter* **1** (1989) 9101.
21. *Idem, Solid State Ionics* **28–30** (1988) 651.
22. L. O. GRIFFIN, "Physical Constants of Linear Homopolymers" (Springer-Verlag, Berlin, 1986).
23. B. L. PARKE, M. A. RATNER and D. F. SHRIVER, *J. Phys. Chem. Solids* **42** (1981) 493.
24. *Idem, J. Electrochem. Soc.* **129** (1982) 1434.
25. M. A. RATNER, in "Polymer Electrolyte Reviews 1", edited by J. R. MacCollum and C. A. Vincent (Elsevier Applied Science, London, New York, 1987) p. 173.

Received 28 June 1991
and accepted 10 January 1992